

An Enhanced Projection Pursuit Tree Classifier with Visual Methods for Assessing Algorithmic Improvements

Natalia da Silva

Dianne Cook

Eun-Kyung Lee

Abstract

This paper presents enhancements to the projection pursuit tree classifier and visual diagnostic methods for assessing their impact in high dimensions. The original algorithm uses linear combinations of variables in a tree structure where depth is constrained to be less than the number of classes—a limitation that proves too rigid for complex classification problems. Our extensions improve performance in multi-class settings with unequal variance-covariance structures and nonlinear class separations by allowing more splits and more flexible class groupings in the projection pursuit computation. Proposing algorithmic improvements is straightforward; demonstrating their actual utility is not. We therefore develop two visual diagnostic approaches to verify that the enhancements perform as intended. Using high-dimensional visualization techniques, we examine model fits on benchmark datasets to assess whether the algorithm behaves as theorized. An interactive web application enables users to explore the behavior of both the original and enhanced classifiers under controlled scenarios. The enhancements are implemented in the R package `PPtreeExt`.

1 Introduction

Loh (2014) provides an extensive overview of decades of research on classification and regression tree algorithms. Tree models are useful because they are simple, yet flexible, fast to compute, widely applicable and interpretable. A main drawback, though, most available methods use splits along single variables, which means that separations best made using a combination of variables are awkward for trees to fit. While there have been many suggestions it is a much harder problem to optimize on linear combinations, and thus there is less available successful software for oblique splits.

One available method and software is the Projection Pursuit Tree (PPtree) algorithm (Y. D. Lee et al. 2013). It optimizes a projection pursuit index, for example the LDA (E.-K. Lee et al. 2005) or PDA (E.-K. Lee and Cook 2010) index among others, based on class information to identify one-dimensional projections that best separate the groups at each node. The PPtree tree structure is simpler than classic methods like `rpart` (Therneau and Atkinson 2025), as it restricts the depth to $G - 1$ (G is the number of classes). At each node, PPtree separates the data into two groups by first deciding which classes to group together;

the data are split into left and right branches based on two group means. This produces a compact and interpretable tree implemented in `PPtreeViz` R package (E.-K. Lee 2018).

One of the main advantages of `PPtree` is its ability to leverage the correlation between predictor variables to improve class separation. It has been shown to outperform even random forests (RF) in some scenarios. Projection pursuit addresses a known limitation of the original RF algorithm, in which oblique projections were allowed. While it sounds appealing, the algorithm is practically infeasible because it is based on randomly generated splits. Thus it is slow, and inefficient, for finding useful separating oblique splits.

The compact nature of `PPtree` means that it fits simply, and does not require pruning. The resulting one-dimensional projections can be used to make visualizations of group separations. However, there are limitations that reduce its effectiveness in certain contexts. Due to the way classes are grouped, the prediction boundaries are often too close to one group, resulting in unnecessarily high error rates. This happens because grouping of classes likely produces unequal variance-covariances, making the pooled variance-covariance used by LDA inadequate. Moreover, when classes have non-elliptical variance-covariance, or are split into multiple clusters, the rigidity of the $(G-1)$ -node structure, will not be sufficiently flexible.

A primary objective of this paper is to describe modifications to the `PPtree` algorithm that address these limitations. The algorithm is changed in two ways: (1) improving prediction boundaries by modifying the choice of split points-through class subsetting; and (2) increasing flexibility by allowing multiple splits per group. The modified algorithm is tested on a variety of benchmark data sets. These data sets include well-separated classes, the presence of outliers, and nonlinear boundaries. The performance is compared with the original `PPtree` algorithm and existing methods. Visual comparisons of decision boundaries, along with error rates, are used to further understand the model fits. The ultimate goal is to provide better building blocks for a projection pursuit-based classification random forest algorithm (da Silva, Cook, and Lee 2021) implemented in `PPforest` R package (da Silva, Cook, and Lee 2025).

Proposing enhancements to algorithms is easy, and theoretically the modifications may seem sensible. In practice, they may not work as one envisions. Thus, an important part of developing algorithm modifications is providing validation that they are doing what is expected. This means going beyond predictive accuracy, to understanding the resulting models. A second objective of this paper is to provide visual diagnostics for the algorithm changes. This is two-fold: a shiny (Chang et al. 2025) app and tours to view the fits in high dimensions. The app is available in the `PPtreeExt` package (da Silva, Cook, and Lee 2026) along with the implementation of the modified algorithm. It allows users to generate 2D data sets with different types of separations and compare the model fits for the modified and the original algorithm. This was an essential tool in constructing the new algorithm, because it provides side-by-side visualization of prediction boundaries to identify data patterns in which the different methods perform better. The second visual diagnostic is to use tours available in the `tourr` package (Wickham et al. 2011) to examine the high-dimensional structure of data sets and the resulting model fits where the modified algorithm outperforms other classifiers. This provides an explanation for the performance comparison results, and intuition for why the modified algorithm performs better.

The paper is organized as follows: Section 2 provides background on the original PPtree algorithm, including its structure and limitations. Section 3 describes the extensions to the algorithm. Section 4 presents the interactive visualization tool developed for exploring and comparing the algorithms. Section 5 presents the comparative analysis of algorithm performance, and visual diagnostics for the comparisons in Section 6. Finally, Section 7 discusses the changes, results of the comparison and potential future directions.

2 Background to PPtree

Figure 1 illustrates the original PPtree algorithm for $G = 3$. Starting from the optimal projection, the green group—having the most distant mean—is relabeled as g_1^* , while the orange and violet groups are combined and relabeled as g_2^* . A second projection vector is then computed using all observations, following the same procedure applied to these two new super-groups. A split point is determined using one of the predefined rules, and observations are assigned to branches by comparing their projected values to the cutoff.

The algorithm computes a split point using one of several methods and the observations are allocated to groups based on whether their projected values fall below or above the cutoff. Since g_1^* contains only one of the original classes, the left branch becomes a terminal node. Because g_2^* still includes two original classes, the procedure is recursively repeated on the right branch.

There are eight different rules available for computing the split point on a given projection. Let \bar{x}_g , x_g^{med} , s_g , IQR_g , and n_g denote the mean, median, standard deviation, interquartile range, and sample size of group g , respectively. Table 1 summarizes the formulas used to calculate the split point value, c , under each rule.

Table 1: Rules for computing the split value, c , between two groups, on a data projection, using means, weighted mean, medians, standard deviations, interquartile ranges.

| Rule | Name | Formula |
|------|----------------------------------|-------------------------------------------------------------------------------------------------------------------------------------|
| 1 | mean | $c = \frac{1}{2}\bar{x}_1 + \frac{1}{2}\bar{x}_2$ |
| 2 | sample size weighted mean | $c = \left(\frac{n_2}{n_1+n_2}\right)\bar{x}_1 + \left(\frac{n_1}{n_1+n_2}\right)\bar{x}_2$ |
| 3 | standard deviation weighted mean | $c = \left(\frac{s_2}{s_1+s_2}\right)\bar{x}_1 + \left(\frac{s_1}{s_1+s_2}\right)\bar{x}_2$ |
| 4 | standard error weighted mean | $c = \frac{s_2/\sqrt{n_2}}{s_1/\sqrt{n_1}+s_2/\sqrt{n_2}}\bar{x}_1 + \frac{s_1/\sqrt{n_1}}{s_1/\sqrt{n_1}+s_2/\sqrt{n_2}}\bar{x}_2$ |
| 5 | median | $c = \frac{1}{2}med_1 + \frac{1}{2}med_2$ |
| 6 | sample size weighted median | $c = \frac{n_2}{n_1+n_2}med_1 + \frac{n_1}{n_1+n_2}med_2$ |
| 7 | IQR weighted median | $c = \frac{IQR_2}{IQR_1+IQR_2}med_1 + \frac{IQR_1}{IQR_1+IQR_2}med_2$ |

| Rule | Name | Formula |
|------|-------------------------------------|-----------------------------------------------------------------------------------------------------------------------------------------|
| 8 | sample size and IQR weighted median | $c = \frac{IQR_2/\sqrt{n_2}}{IQR_1/\sqrt{n_1}+IQR_2/\sqrt{n_2}}med_1 + \frac{IQR_1/\sqrt{n_1}}{IQR_1/\sqrt{n_1}+IQR_2/\sqrt{n_2}}med_2$ |

2.1 Algorithm

The PPtree algorithm (Y. D. Lee et al. 2013) follows a multi-step procedure to identify linear combinations of predictors that optimally separate classes in multi-class settings. Let $d_n = \{(x_i, y_i)\}_{i=1}^n$ denote the dataset, where x_i is a p -dimensional vector of explanatory variables. The corresponding class label is $y_i \in \mathcal{G}$, with $\mathcal{G} = \{1, 2, \dots, G\}$, for $i = 1, \dots, n$. The construction of a PPtree classifier follows a four-step algorithm, described as follows:

PPtree Algorithm (4-step version)

Input: Dataset $d_n = \{(x_i, y_i)\}_{i=1}^n$, with $x_i \in \mathbb{R}^p$, $y_i \in \mathcal{G} = \{1, \dots, G\}$

Output: A projection pursuit classification tree with at most $G - 1$ internal nodes

- Step 1: Class Separation. Optimize a projection pursuit index (e.g., LDA or PDA) to find a projection vector α that best separates all classes in the current node.
- Step 2: Binary Relabeling. On projected data, $z_i = \alpha^T x_i$, compute projected class means $\bar{z}_1, \dots, \bar{z}_G$. Identify the pair with the largest mean difference and compute the midpoint mp . Relabel the observations into two super-classes, g_1^* and g_2^* , depending on whether \bar{z}_g is smaller than the midpoint mp .
- Step 3: Node Splitting. Optimize a new projection α^* to separate g_1^* and g_2^* based on the relabeled classes. Define the split value c on $z_i^* = \alpha^{*T} x_{g_i^*}$ using a predefined rule (e.g., mean or weighted mean). Split the node using the rule $z_i^* < c$.
- Step 4: Recursive Partitioning. Repeat Steps 1–3 for each child node until every terminal node contains only one original class.

2.2 Less desirable aspects

The decision boundaries of a classifier reflect how the model partitions the feature space and adapt to class separations. Visualizing the decision boundaries provides valuable insights into model behavior and limitations. To illustrate the motivation for extending the PPtree algorithm, we present simple examples based on simulated datasets. Details on the simulation settings are provided in Section 4.

Figure 2 shows the decision boundaries produced by `rpart` (left) and `PPtree` (right). In this example, the class structure is best separated using linear combinations of the two variables. The `rpart` algorithm, which relies on axis-aligned splits, must approximate the ideal boundary using multiple steps. In contrast, `PPtree` generates an oblique split that more effectively captures the separation, although the resulting boundary between the orange and purple classes lies too close to one of them.

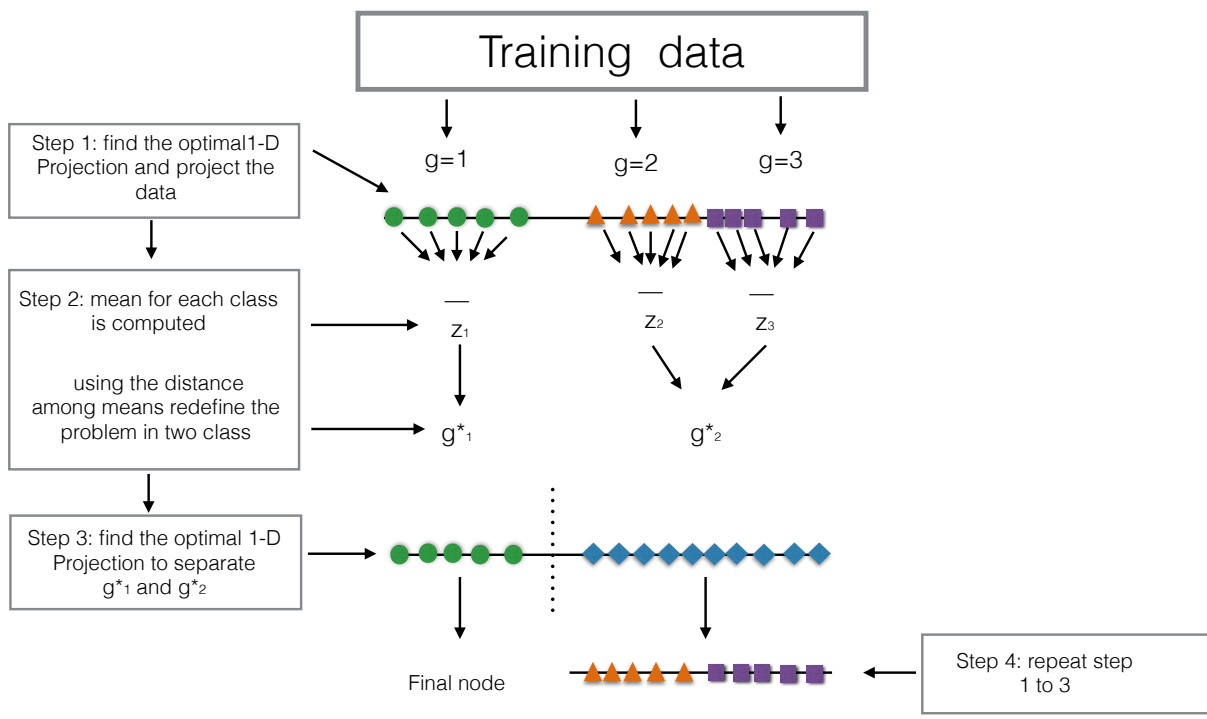


Figure 1: Illustration of the original PPtree algorithm for $G = 3$.

The first split isolates the violet class from the other two. A second partition then attempts to separate the green and orange groups. Although the group structure is similar across the three classes, the resulting decision boundaries are not parallel. This occurs because the initial split uses the combined information from the orange and green groups—treated as a super-group—to compute the projection and determine the splitting point.

Alternative rules for computing the split value (see Table 1) have a substantial impact on the position and orientation of these decision boundaries.

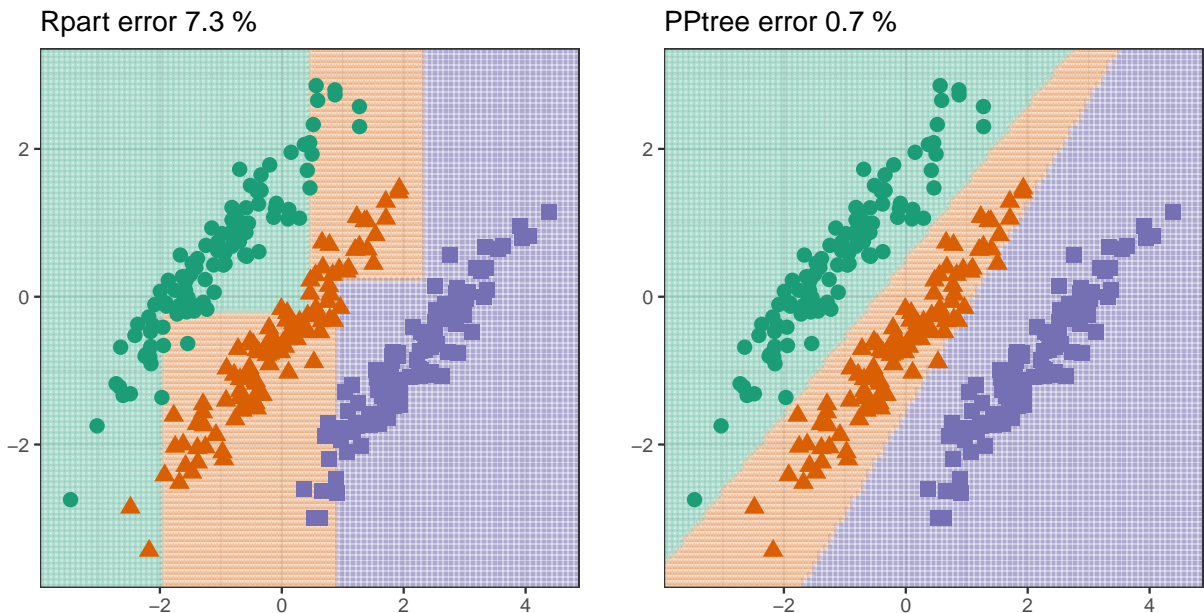


Figure 2: Comparison of decision boundaries produced by the `rpart` (left) and `PPtree` (right) algorithms on two-dimensional simulated data. The boundaries generated by `PPtree` are oblique to the coordinate axes, capturing the linear association between the two variables.

Figure 3 displays a simulated example that highlights the limited flexibility of the decision boundaries produced by `PPtree`. In this scenario, the orange class cannot be separated using a single linear partition, and `PPtree` fails to model it accurately because each original class must be assigned to a single terminal node. In contrast, the more traditional `rpart` algorithm performs better in this case, as its recursive structure allows it to accommodate the relatively simple non-linear separation.

3 PPtree extensions

The algorithm has been extended in two main ways: by modifying the rules used to determine decision boundaries and by allowing multiple splits per group. Two new approaches are

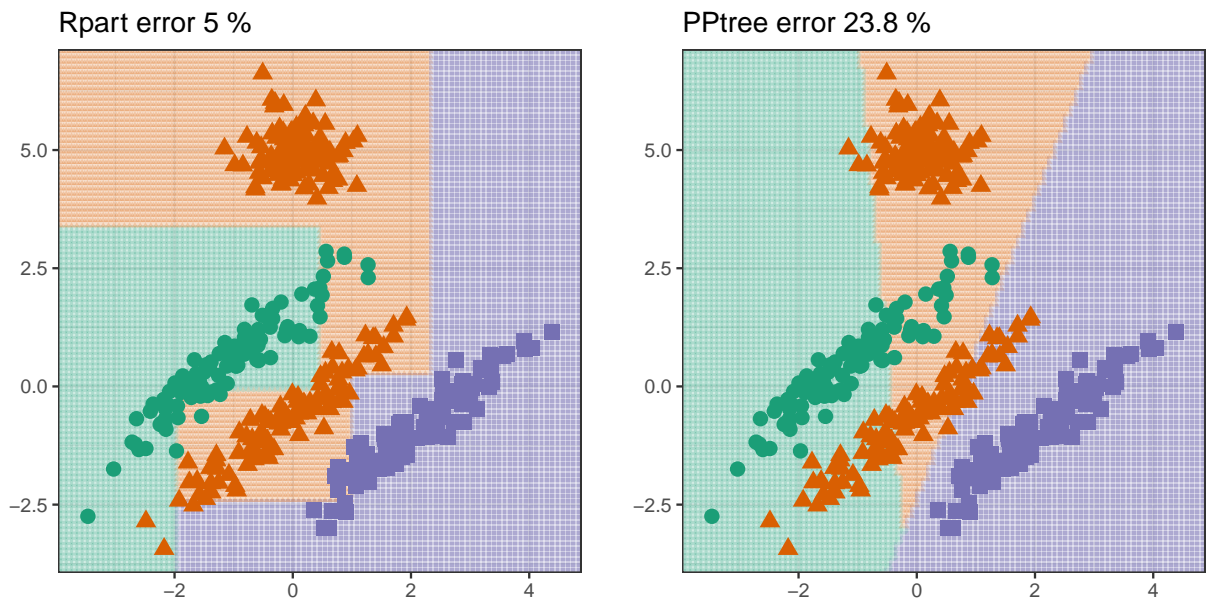


Figure 3: Comparison of decision boundaries produced by the `rpart` (left) and `PPtree` (right) algorithms on two-dimensional simulated data. The orange class cannot be separated using a single linear partition, and `PPtree` fails to model it accurately because each original class must be assigned to a single terminal node.

introduced for computing the optimal split value. To support multiple splits within a group, additional stopping rules must be incorporated into the algorithm.

3.1 Modification 1: Subsetting classes to produce better boundaries

The first modification targets the third step of the original algorithm. Rather than combining all remaining classes into a single super-class, only the two closest ones—identified by the smallest difference in their projected means—are used to compute the next projection and define the split point

3* Find an optimal one-dimensional projection α^{**} , using a subset of $\{(x_i, y_i^*)\}_{i=1}^n$ to separate the two class problem g_1^* and g_2^* . To this second projection only information from the two closest groups, one from g_1^* and the other from g_2^* are used. The best separation of g_1^* and g_2^* is determined by $\alpha^{*T} \bar{x}_{g_1^*} < c$; then g_1^* is assigned to the left node else assign g_2^* to the right node, where $\bar{x}_{g_1^*}$ is the mean of g_1^* .

Figure 4 illustrates the modified version of the algorithm for a three-class classification problem. After identifying the initial optimal projection, instead of combining two groups into a single super-group, the group furthest from the others is temporarily excluded. In this example, class g_3 is dropped from the current node. A new projection is then computed using only classes g_1 and g_2 (reabeled as g_1^* and g_2^*), and one of the eight available rules is applied to determine the optimal split point. Subsequently, class g_3 is reintroduced, and a new projection is computed to best separate it from g_2 , completing the tree construction.

Figure 6 shows the effect of this modification on the decision boundaries obtained from the simulated dataset presented in Figure 2.

3.2 Modification 2: Multiple splits per class based on entropy reduction

This modification introduces a new approach for selecting the split value, based on the impurity of the resulting groups. This approach resembles the impurity-based criteria used in the `rpart` algorithm, but it operates on projected data rather than individual features. Currently, the only implemented impurity measure is negative entropy:

$$E(s) = - \sum_{j=1}^G p_{js} \log(p_{js}) \quad (1)$$

where p_{js} is the proportion of observations from class j in subset s , and G is the number of classes. Higher values of $E(s)$ indicate greater class impurity. When all observations in the subset belong to the same class, the entropy reaches its minimum value of $E(s) = 0$, indicating a pure node. To evaluate the quality of a candidate split, the impurity values of the resulting left and right subsets are combined using a weighted average of the entropies:

$$E(s_L, s_R) = \frac{n_L}{n_L + n_R} E(s_L) + \frac{n_R}{n_L + n_R} E(s_R) \quad (2)$$

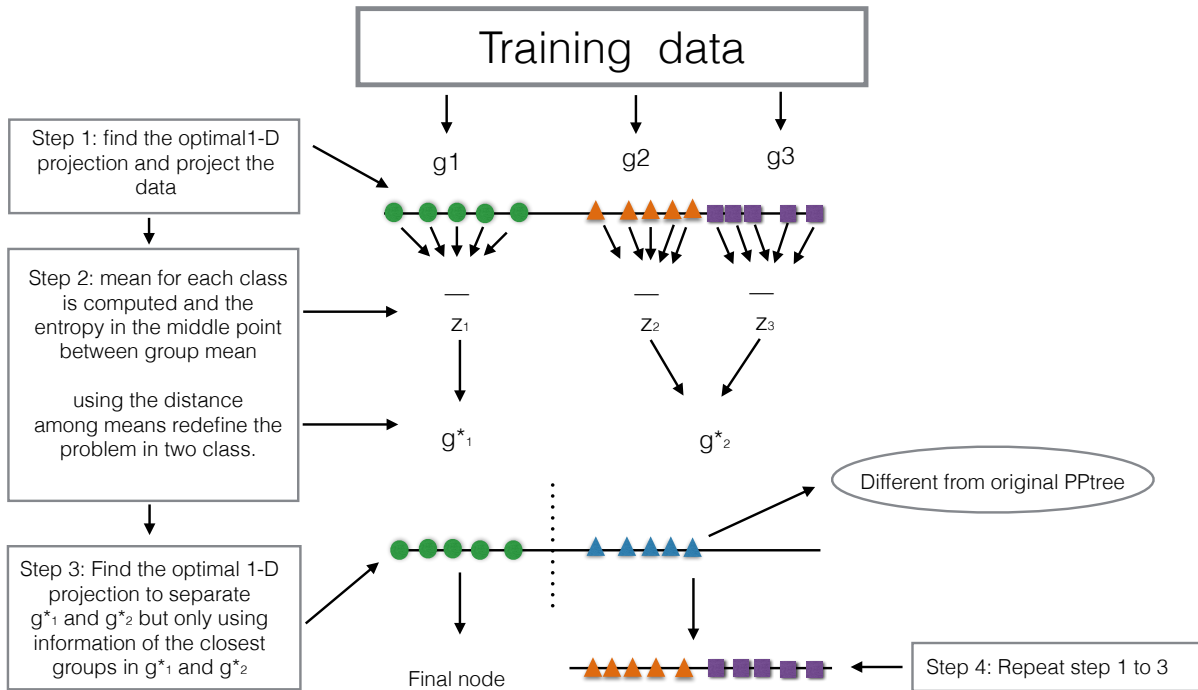


Figure 4: Illustration of the algorithm with Modification 1 applied to a three-class problem. At each node, the second one-dimensional projection is computed using only the two closest groups to determine the best projection direction and split point.

where n_L, n_R are the number of observations in the left and right subsets, respectively. The combined impurity, $E(s_L, s_R)$ is computed for all possible split points—defined as the midpoints between consecutive ordered projected values—denoted $\mathcal{C} = \{c_1, \dots, c_{n_L+n_R-1}\}$. The split point that minimizes the combined entropy is selected:

$$\min_{c \in \mathcal{C}} E_c(s_L, s_R)$$

This represents a major departure from the original PPtree structure, aiming to enhance flexibility in modeling non-linear class boundaries by allowing multiple splits within a class. Instead of relying on summary statistics at the class level, this approach shifts the focus to local differences between individual observations. To support this flexibility, additional control mechanisms are required, particularly new stopping criteria. While this is conceptually similar to the `rpart` algorithm, a key distinction is that larger sample sizes per node are needed to reliably estimate projection coefficients.

Figure 5 illustrates this modified version of the algorithm, which follows the steps outlined below.

PPtree Algorithm with Entropy-Based Splitting

Input: Dataset $d_n = \{(x_i, y_i)\}_{i=1}^n$, with $x_i \in \mathbb{R}^p$, $y_i \in \mathcal{G} = \{1, \dots, G\}$

Output: A projection pursuit classification tree with entropy-based node splitting

- Step 1: Class Separation. Optimize a projection pursuit index (e.g., LDA or PDA) to find a projection vector α that best separates the classes in the current node.
- Step 2: Projection and Candidate Splits. On the projected data, $z_i = \alpha^T x_i$, define candidate splits as midpoints between consecutive z_i values.
- Step 3: Impurity Evaluation. For each candidate split c , divide the data into $s_L = \{z_i < c\}$ and $s_R = \{z_i \geq c\}$. Compute the class proportions p_{js} for each subset and evaluate the entropy:

$$E(s) = - \sum_{j=1}^G p_{js} \log(p_{js})$$

Compute the total impurity as:

$$E(s_L, s_R) = \frac{n_L}{n_L + n_R} E(s_L) + \frac{n_R}{n_L + n_R} E(s_R)$$

- Step 4: Best Split Selection. Select the split point c^* that minimizes $E(s_L, s_R)$. Split the node using the rule $z_i < c^*$.
- Step 5: Recursive Partitioning. Repeat Steps 1–4 recursively on each child node until some of the following stopping criteria are met:
 - All observations in the node belong to the same class;

- The node size is smaller than a minimum threshold n_s ;
- The entropy reduction is smaller than a threshold ent_s .

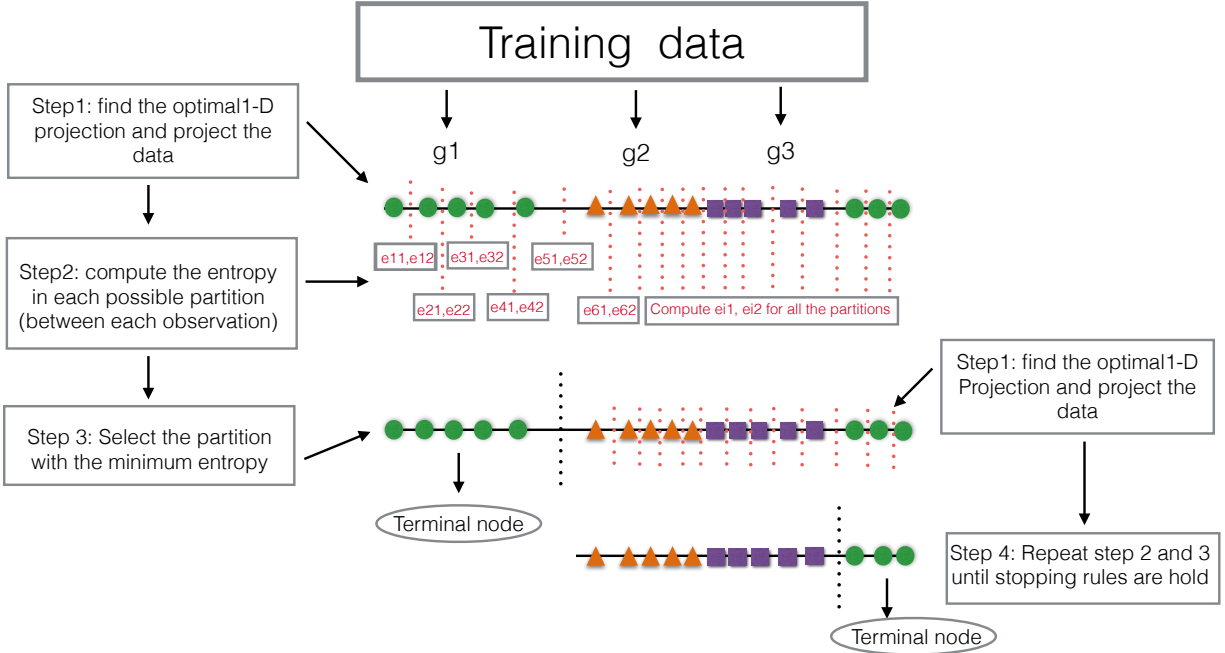


Figure 5: Illustration of the algorithm with Modification 2 applied to a three-class problem. Projections of the data are computed at each node, and multiple splits per class are allowed. An impurity-based criterion, such as entropy, is used to determine when and how often to split observations within a node.

4 Algorithm comparison

To evaluate both the original algorithm and the proposed modifications, we developed an interactive Shiny app (Chang et al. 2025). The tool includes methods for simulating 2D classification problems, and displays the decision boundaries generated by different algorithms: CART, PPtree, and the proposed extensions (implemented in `rpart`, `PPtreeViz`, and `PPtreeExt`, respectively). The Shiny app is available at <https://natyds.shinyapps.io/explorapp/> and is implemented in `PPtreeExt`.

The app contains three tabs, each tab offers control over data generation and algorithm parameters: Basic-Sim, Sim-Outlier, and MixSim. The first tab simulates well-separated

classes, the second includes a cluster of outliers, and the third generates overlapping groups using the `MixSim` package (Melnykov, Chen, and Maitra 2012). Each tab offers control over data generation and algorithm parameters. The decision boundaries for `rpart`, `PPtree`, and the modified `PPtree` are displayed side by side for visual comparison.

Additional controls, such as the rule partition used in `PPtree` algorithm and the modified `PPtree` based on subsetting classes, can be incorporated into the application. These features allow users to examine how changes in rule criteria influence the resulting classification boundaries.

Figure 6 illustrates the use of the interactive application. The first modification (Subsetting classes) is applied to generate the projection, and Rule 1 is used to compute the split point. The modified `PPtree` achieves an error rate comparable to the original `PPtree`, with both substantially outperforming `rpart`. Additionally, the resulting decision boundary more accurately partitions the groups in a balanced manner.

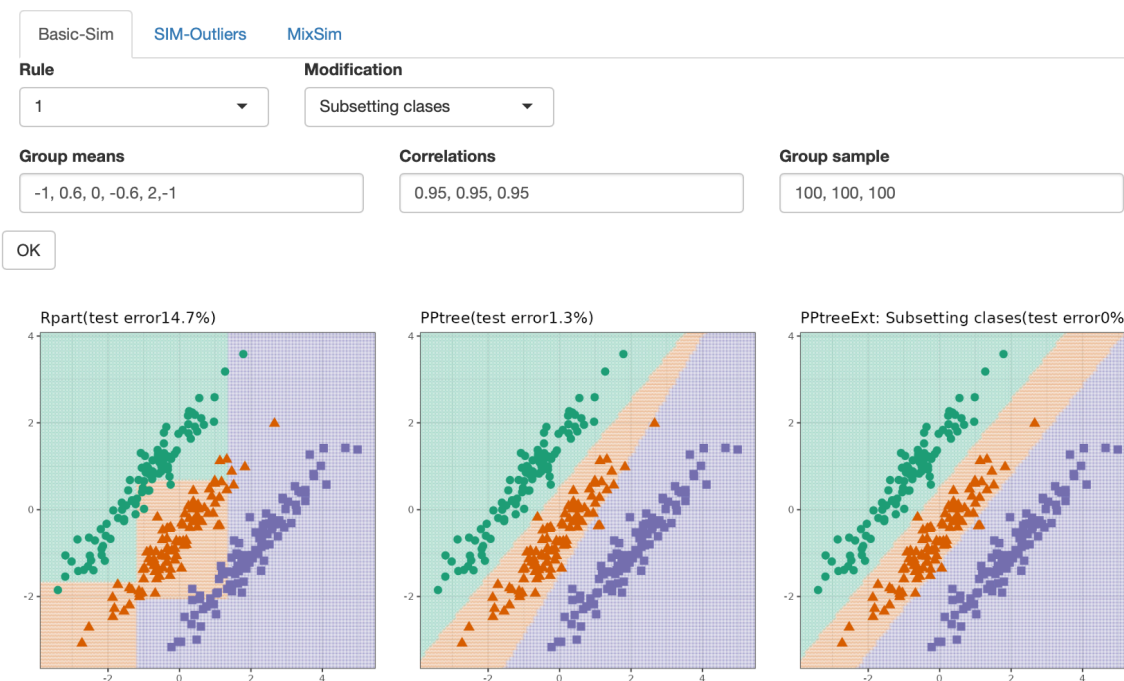


Figure 6: Model fits for the three algorithms—`rpart`, `PPtree`, and the modified `PPtree` based on subsetting classes applied to simulated well-separated classes. For `PPtree`, Rule 1 is used to determine the split points. The modified `PPtree` produces decision boundaries that are more symmetrically placed between the clusters.

Figure 7 presents a scenario in which Modification 2 (Multiple splits) yields a substantial improvement over the other algorithms. The use of multiple splits enables the small group of outliers from class 2 to be correctly classified.

Figure 8 compares the performance of the algorithm variants on data simulated from Gaussian mixtures. The user can adjust several parameters of the mixture model: n is the sample

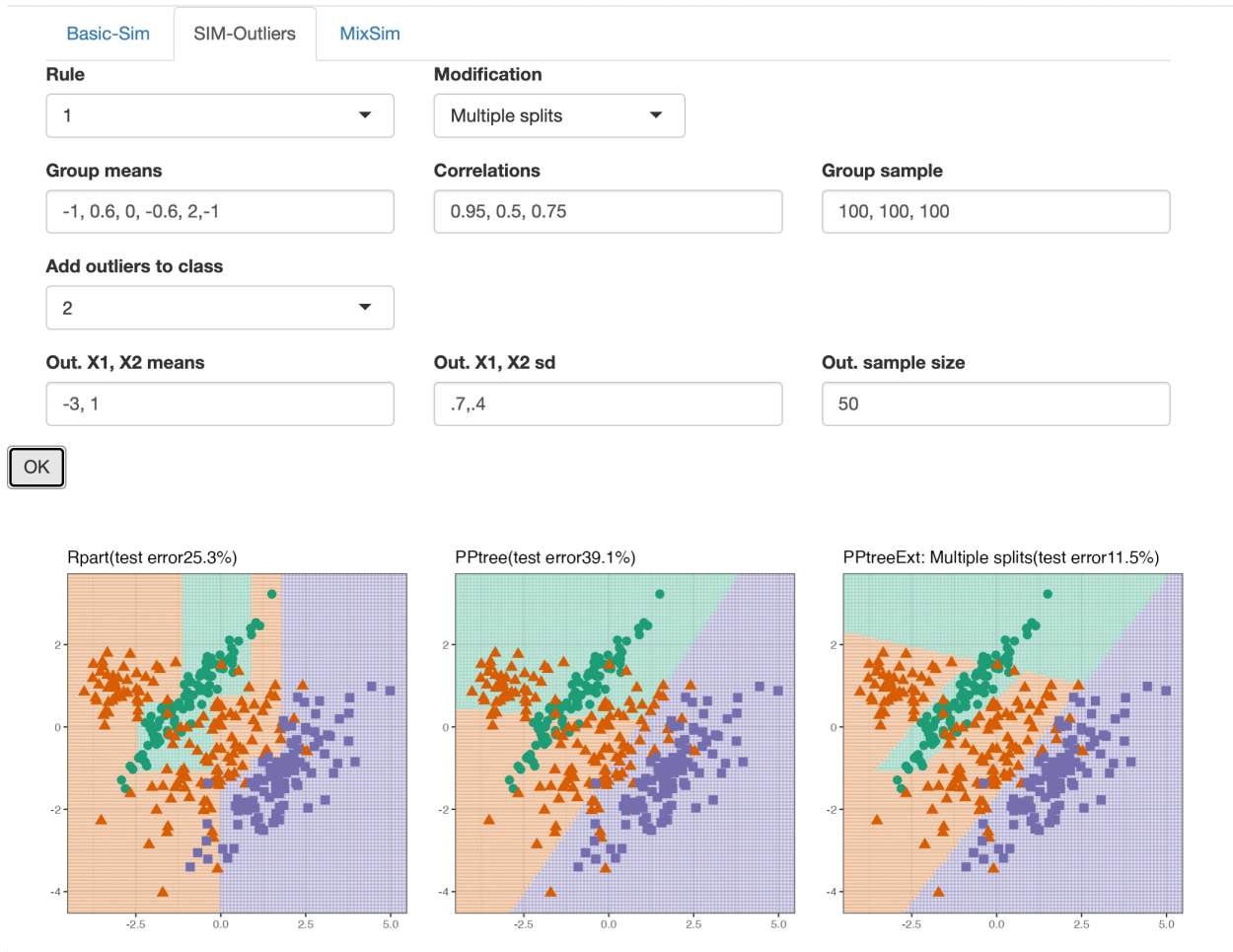


Figure 7: Model fits for the three algorithms—rpart, PPtree, and the modified PPtree—applied to data in which one class consists of two distinct clusters. The boundaries produced by the modified PPtree with multiple splits better capture the underlying structure of the data compared to the other methods.

size, $BarOmega$ is the desired average overlap between components, $MaxOmega$ specifies the maximum allowable overlap, and K is the number of groups.



Figure 8: Decision boundaries produced by the three algorithms— rpart, PPtree, and the modified PPtree—on data simulated from a Gaussian mixture model.

The interactive application provides insight into how modifications to the algorithm affect model fit. It follows the principle of visualizing the model in the data space (Wickham, Cook, and Hofmann 2015). An additional and important use of the tool has been for debugging and evaluating the algorithmic behavior. By adjusting the simulated data and model parameters, it becomes evident that small changes in the data can result in substantial changes in the fitted model—particularly when projections are involved.

This sensitivity is likely to be even greater in higher-dimensional settings. However, in scenarios where class separation occurs along combinations of variables, the use of projected data at each node tends to yield decision boundaries that more closely align with the true data distribution.

5 Performance comparison

This section presents a benchmark data study to evaluate the predictive performance of the proposed method. We compare the extended PPtree models with several classification methods—CART, PPtree, Random Forest, PPforest, and SVM—using 94 benchmark datasets. Table 3 in the Appendix contain the url with the source data while Table 6 summarize the main characteristics of each dataset summarizing the number of observations, predictors, number of classes, class imbalance, and absolute average correlation among predictors. Imbalance quantifies the disparity in class sizes (0 indicates perfectly balanced classes, biggest proportion size difference between classes), while higher correlation suggests a greater potential for class separation through linear combinations of variables.

For each dataset, two-thirds of the observations are randomly selected for training, and the remaining one-third is used for testing and computing the prediction error. This process is repeated 200 times.

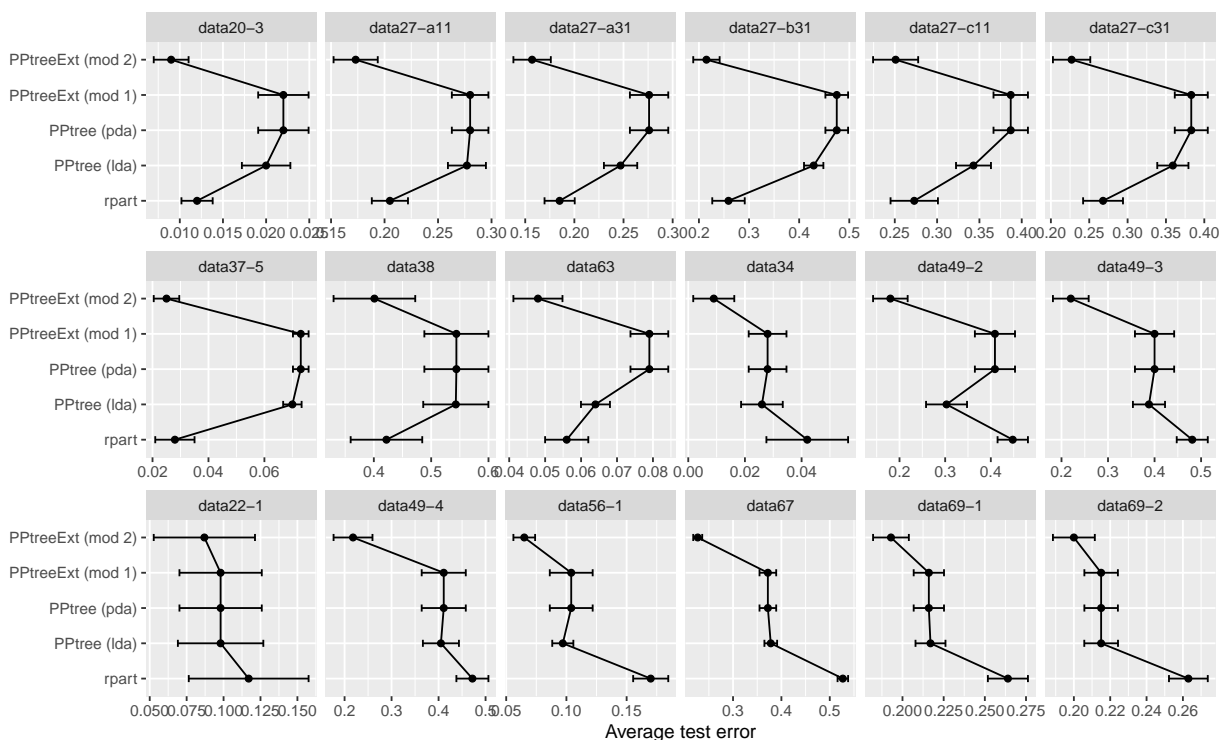


Figure 9: Average test error from 200 training/test splits of benchmark data for four models: rpart, PPtree PPtreeExt modifications 1 and 2, where the PPtree extension performs better than rpart and the original PPtree.

Moreover, in 18 datasets, the modified PPtree outperforms CART, as illustrated in Figure 9, and in only 3 cases it achieves the lowest error among all selected methods, including ensemble-based classifiers. Table 2 presents an overview of these datasets, which is a subset of Table 6 from the Appendix.

Table 2: Overview of benchmark datasets where the proposed tree-based extensions outperform the selected tree methods. The table summarizes the number of observations, predictors, number of classes, class imbalance, and absolute average correlation among predictors. Imbalance quantifies the disparity in class sizes (0 indicates perfectly balanced classes), while higher correlation suggests a greater potential for class separation through linear combinations of variables.

| dataset | Cases | Predictors | Groups | Imbalance | Correlation |
|------------|-------|------------|--------|-----------|-------------|
| data20-3 | 8143 | 5 | 2 | 0.58 | 0.45 |
| data27-a11 | 1747 | 18 | 5 | 0.38 | 0.24 |
| data27-a31 | 1834 | 18 | 5 | 0.28 | 0.27 |
| data27-b31 | 1424 | 18 | 5 | 0.21 | 0.24 |
| data27-c11 | 1111 | 18 | 5 | 0.14 | 0.27 |
| data27-c31 | 1448 | 18 | 5 | 0.17 | 0.27 |
| data37-5 | 17560 | 53 | 5 | 0.21 | 0.16 |
| data38 | 182 | 12 | 2 | 0.43 | 0.21 |
| data63 | 6598 | 166 | 2 | 0.69 | 0.27 |
| data34 | 1372 | 4 | 2 | 0.11 | 0.43 |
| data49-2 | 606 | 100 | 2 | 0.03 | 1.00 |
| data49-3 | 606 | 100 | 2 | 0.01 | 0.99 |
| data22-1 | 258 | 5 | 4 | 0.25 | 0.12 |
| data49-4 | 606 | 100 | 2 | 0.01 | 0.99 |
| data56-1 | 7494 | 16 | 10 | 0.01 | 0.27 |
| data67 | 20000 | 16 | 26 | 0.00 | 0.18 |
| data69-1 | 5000 | 21 | 3 | 0.01 | 0.30 |
| data69-2 | 5000 | 40 | 3 | 0.01 | 0.09 |

6 Explanation of performance

We would expect that the modified PPtree algorithm outperforms

- rpart when the best separation between groups is in oblique directions
- and the original PPtree when class variances are different, or when there are multiple classes.

This can be investigated visually using a tour. There are several strategies for approaching this:

1. On the data
 - a. Work on two groups at a time, if there are more than 2
 - b. Use a guided tour on the data to find the combinations of the variables where the groups are separated
2. Predict a grid of values that covers the data domain, for the methods interested in comparing, PPtreeExt, rpart and PPtree
 - a. subset to the points near the border generated by the classifier.

- b. record a sequence of projection bases that shows the boundary created by PPtree
- c. use the same projection sequence to view the boundaries for the three different methods, possibly use a slice tour to focus on the boundary near the center of the data domain.

Figure 10 show projections of the `data20-3` illustrating why PPtreeExt performs better. Group 0 is split on either side of group 1, which means that the original PPtree algorithm would not be able to capture both clusters. We can also see that the separation is mostly on `V3` but small amounts of other variables help to improve the separation. This means that `rpart` will not work quite as well because it will focus on splitting `V3`.

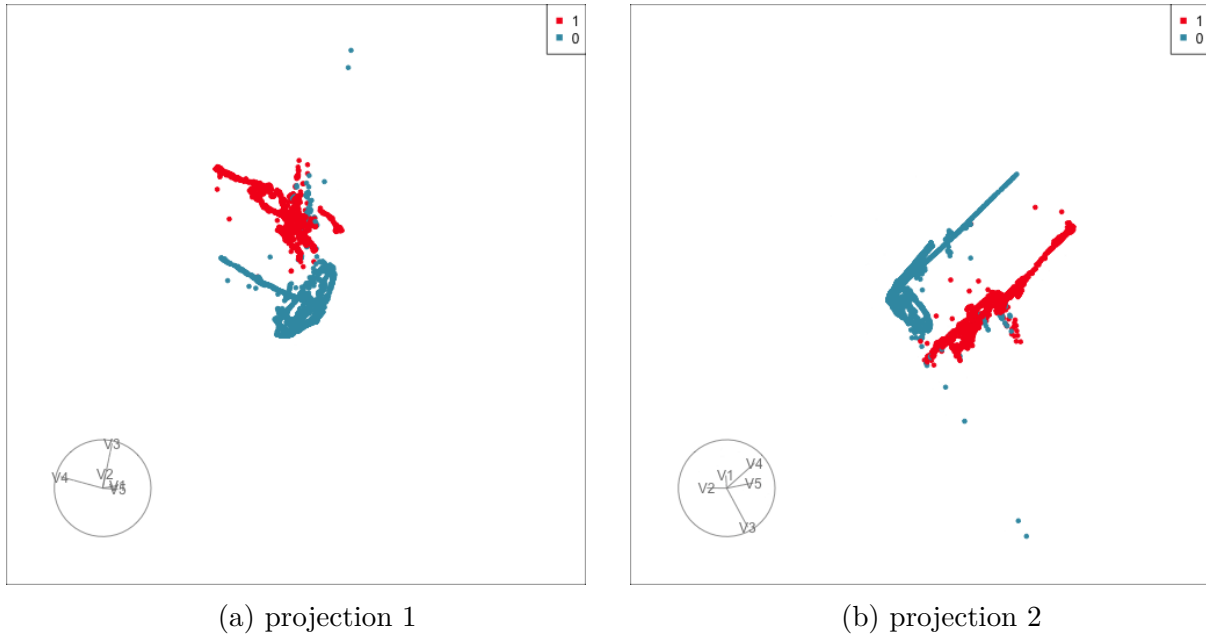


Figure 10: Two projections from a grand tour of `data20-3`, from which we can see why the PPtreeExt method is the most effective. The group 0 is split into two clusters on either side of group 1, which means that the original algorithm is not optimal. Secondly, the separation between the two groups is in a combination of variables.

Figure 11 shows some plots illustrating why PPtreeExt outperforms the other methods of the `data49-2` data. From Figure 9 we can see that the original PPtree (with LDA) algorithm performs much better than a tree, and the PPtreeExt performs much better again. This data has 100 predictors and 2 classes (Table 2), which makes visualising more challenging than `data20-3`. A useful approach is to pre-process using principal component analysis (PCA) on the predictors, to reduce the number of variables to visualise, while maintaining class structure. Plot (a) shows PC 1 vs PC2, with points coloured by the two classes. PC 1 explains 99.8% of the variability in the predictors but it explains nothing of the class structure. This is not uncommon for PCA, where often interesting structure can be found in the smaller components. Plot (b) shows PC 2 vs PC 3, and here we see interesting class differences. Each class appears to have three linear pieces pointing in different directions. This supports why PPtreeExt might work well, because in the combination of variables, the

classes are nearly separable with multiple linear cuts. It's not feasible to continue working through principal components to tease apart the cluster structure relating to classes, so a good next step is to do projection pursuit. The optimal projection is shown in plot (c). It can be seen the two classes are mostly separable by a linear combination of variables, but there is no gap between the clusters. The linear combination with so many variables is what causes some difficulties for a simple tree algorithm. The interesting shapes of the clusters for each class, which appear to be multiple linear pieces, means that the PPtreeExt can find better separations than PPtree.

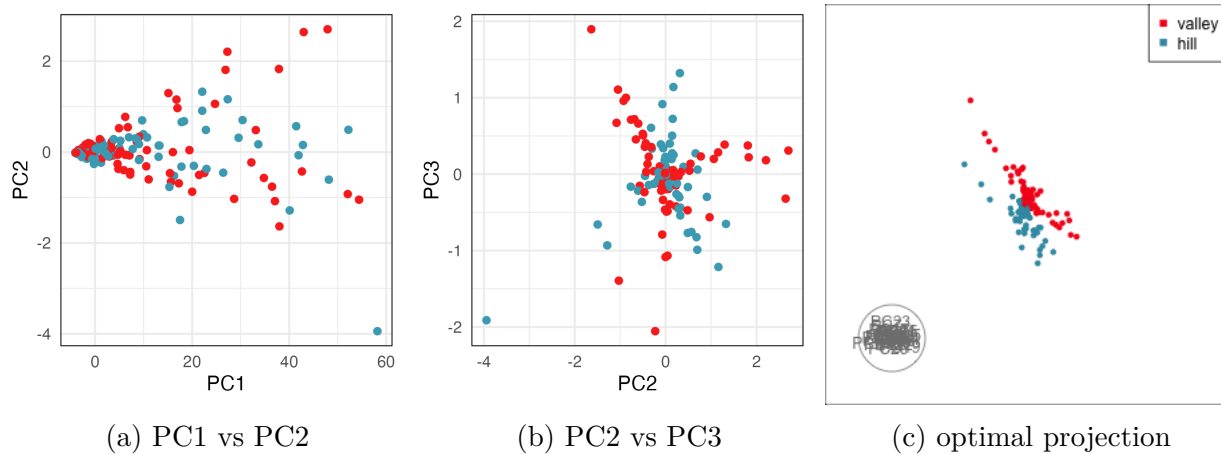


Figure 11: Examining why `data49-2` is best classified using PPtreeExt. Because there are 100 predictors, for visualisation it is useful to reduce the dimension using principal component analysis, and then examine the separation between groups. PC1 explains 99.8% of the overall variability among predictors, but it is not useful for separating the classes (a). PC2 and PC3 (b) have an interesting difference between the two classes which shows why multiple linear splits might be useful. A guided projection pursuit on the first 26 principal components (c) shows that these classes could be separated with a linear combination. This is why the original PPtree classifier does better than the tree algorithm and also why the extension improves the performance.

Figure 12 has plots illustrating why the PPtreeExt performs better on `data69-1`. From Figure 9 we see that all of the PPtree versions perform better than an `rpart` fit. This data has 21 predictors and 3 classes (Table 2). This is sufficiently small to examine using a tour, and we initially use a guided tour with the LDA index. This produced the projection shown in plot (a) where we see the primary difference between the three classes. These are each similar size, but oriented in such a way that in a 2D projection they form a triangle. Plots (b) and (c) show the boundaries using a slice tour with the same projection as used in (a) for PPtreeExt and `rpart`, respectively. The boundary points are generated by simulating a random sample of observations between $(-3, 3)$ in each dimension. The slice cuts through to centre of the box. We can see that PPtreeExt essentially fits the data shape neatly but the `rpart` boundary is very messy. This data needs oblique cuts, which PPtreeExt provides, and the modified algorithm handles the variance differences better than the original.

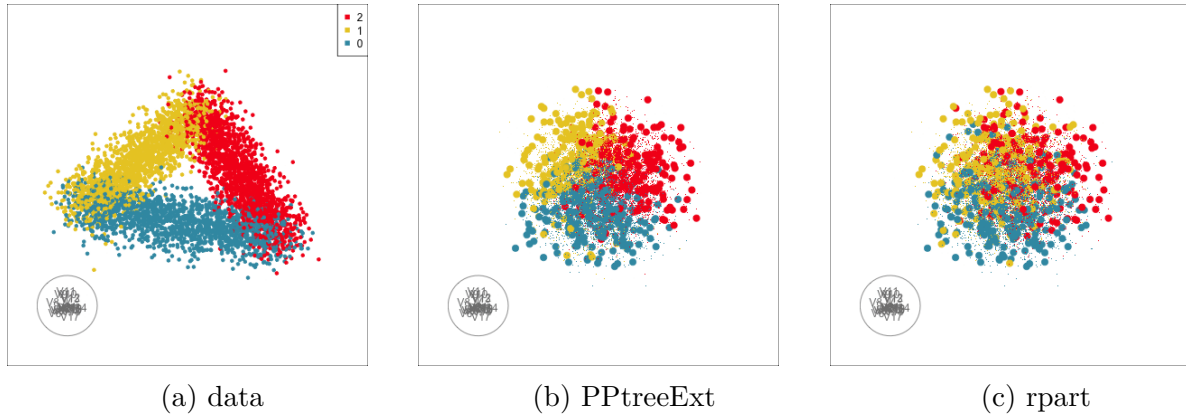


Figure 12: Examining why `data49-2` is best classified using `PPtreeExt`: (a) best projection from a guided tour shows that the data has three similar linear pieces oriented to form a triangle, (b) boundary produced by the `PPtreeExt` fitted model and (c) boundary produced by `rpart` fitted model.

7 Discussion

This article has presented two modifications to the `PPtree` algorithm for classification problems implemented in the R package `PPtreeExt` and evaluated using a purpose-built interactive web application and real data. The first modification involves subsetting classes when calculating the projection direction at each node, while the second allows for multiple splits per class based on individual entropy evaluations between candidate splits. These changes result in a more flexible classification method that leverages linear combinations of variables. The web application also demonstrates how easily diagnostic tools can be constructed to explore and understand the behavior of new algorithms.

The benchmark data study showed that `PPtreeExt` predictive performance is better than, `CART` and `PPtree` in 18 data out of 94. The modified `PPtree` algorithm outperforms `CART` in cases when the best separation between groups is in oblique directions and outperforms the original `PPtree` when class variances are different, or when there are multiple classes.

Interpretability is increasingly important, because predictions from algorithms may need to be defended in practice. We have shown how to examine the data and the fitted model to understand why the `PPtree` extension performs better than other tree methods on some data sets. This approach is generally useful for assessing and diagnosing model fits.

The modified tree algorithm can be incorporated into a projection pursuit forest classifier (da Silva, Cook, and Lee 2025). Given its implicit variable selection mechanism, the ensemble is expected to handle nuisance variables more effectively than a single tree. Additionally, the use of bagging should yield improved and more robust performance in problems with nonlinear decision boundaries. This can be accomplished using the current `PPforest` package.

8 Appendix

Table 3: Source data information

| Name | URL |
|------------|-----------------------------------------------------------------------------------------------------------------------------------------------------------------------------|
| data12 | https://archive.ics.uci.edu/dataset/518/speaker+accent+recognition |
| data13-1 | https://archive.ics.uci.edu/dataset/547/algerian+forest+fires+dataset |
| data13-2 | https://archive.ics.uci.edu/dataset/547/algerian+forest+fires+dataset |
| data20-1 | https://archive.ics.uci.edu/dataset/357/occupancy+detection |
| data20-2 | https://archive.ics.uci.edu/dataset/357/occupancy+detection |
| data20-3 | https://archive.ics.uci.edu/dataset/357/occupancy+detection |
| data21 | https://archive.ics.uci.edu/dataset/537/cervical+cancer+behavior+risk |
| data22-1 | https://archive.ics.uci.edu/dataset/257/user+knowledge+modeling |
| data22-2 | https://archive.ics.uci.edu/dataset/257/user+knowledge+modeling |
| data26 | https://archive.ics.uci.edu/dataset/308/gas+sensor+array+under+flow+modulation |
| data27-a11 | https://archive.ics.uci.edu/dataset/302/gesture+phase+segmentation |
| data27-a21 | https://archive.ics.uci.edu/dataset/302/gesture+phase+segmentation |
| data27-a31 | https://archive.ics.uci.edu/dataset/302/gesture+phase+segmentation |
| data27-a32 | https://archive.ics.uci.edu/dataset/302/gesture+phase+segmentation |
| data27-b11 | https://archive.ics.uci.edu/dataset/302/gesture+phase+segmentation |
| data27-b12 | https://archive.ics.uci.edu/dataset/302/gesture+phase+segmentation |
| data27-b31 | https://archive.ics.uci.edu/dataset/302/gesture+phase+segmentation |
| data27-b32 | https://archive.ics.uci.edu/dataset/302/gesture+phase+segmentation |
| data27-c11 | https://archive.ics.uci.edu/dataset/302/gesture+phase+segmentation |
| data27-c12 | https://archive.ics.uci.edu/dataset/302/gesture+phase+segmentation |
| data27-c31 | https://archive.ics.uci.edu/dataset/302/gesture+phase+segmentation |
| data27-c32 | https://archive.ics.uci.edu/dataset/302/gesture+phase+segmentation |
| data29 | https://archive.ics.uci.edu/dataset/282/lsvt+voice+rehabilitation |
| data32 | https://archive.ics.uci.edu/dataset/257/user+knowledge+modeling |
| data34 | https://archive.ics.uci.edu/dataset/267/banknote+authentication |
| data36 | https://archive.ics.uci.edu/dataset/236/seeds |
| data37-1 | https://archive.ics.uci.edu/dataset/231/pamap2+physical+activity+monitoring |
| data37-2 | https://archive.ics.uci.edu/dataset/231/pamap2+physical+activity+monitoring |
| data37-3 | https://archive.ics.uci.edu/dataset/231/pamap2+physical+activity+monitoring |
| data37-4 | https://archive.ics.uci.edu/dataset/231/pamap2+physical+activity+monitoring |
| data37-5 | https://archive.ics.uci.edu/dataset/231/pamap2+physical+activity+monitoring |
| data37-8 | https://archive.ics.uci.edu/dataset/231/pamap2+physical+activity+monitoring |
| data37-14 | https://archive.ics.uci.edu/dataset/231/pamap2+physical+activity+monitoring |
| data38 | https://archive.ics.uci.edu/dataset/230/planning+relax |
| data39-1 | https://archive.ics.uci.edu/dataset/224/gas+sensor+array+drift+dataset |

| Name | URL |
|----------|-------------------------------------------------------------------------------------------------------------------------------------------------------------|
| data39-2 | https://archive.ics.uci.edu/dataset/224/gas+sensor+array+drift+dataset |
| data39-3 | https://archive.ics.uci.edu/dataset/224/gas+sensor+array+drift+dataset |
| data39-4 | https://archive.ics.uci.edu/dataset/224/gas+sensor+array+drift+dataset |
| data39-5 | https://archive.ics.uci.edu/dataset/224/gas+sensor+array+drift+dataset |
| data39-6 | https://archive.ics.uci.edu/dataset/224/gas+sensor+array+drift+dataset |
| data39-7 | https://archive.ics.uci.edu/dataset/224/gas+sensor+array+drift+dataset |

data39-8 <https://archive.ics.uci.edu/dataset/225/gas+sensor+array+drift+dataset>
data39-9 <https://archive.ics.uci.edu/dataset/226/gas+sensor+array+drift+dataset>
data41-1 <https://archive.ics.uci.edu/dataset/194/wall+following+robot+navigation+data>
data41-2 <https://archive.ics.uci.edu/dataset/194/wall+following+robot+navigation+data>
data41-3 <https://archive.ics.uci.edu/dataset/194/wall+following+robot+navigation+data>
data42 <https://archive.ics.uci.edu/dataset/192/breast+tissue>
data44 <https://archive.ics.uci.edu/dataset/181/libras+movement>
data49-2 <https://archive.ics.uci.edu/dataset/167/hill+valley>
data49-3 <https://archive.ics.uci.edu/dataset/168/hill+valley>
data49-4 <https://archive.ics.uci.edu/dataset/169/hill+valley>
data50 <https://archive.ics.uci.edu/dataset/161/mammographic+mass>
data52-1 <https://archive.ics.uci.edu/dataset/96/spectf+heart>
data52-2 <https://archive.ics.uci.edu/dataset/96/spectf+heart>
data53 <https://archive.ics.uci.edu/dataset/139/synthetic+control+chart+time+series>
data55-1 <https://archive.ics.uci.edu/dataset/80/optical+recognition+of+handwritten+digits>
data55-2 <https://archive.ics.uci.edu/dataset/80/optical+recognition+of+handwritten+digits>
data56-1 <https://archive.ics.uci.edu/dataset/81/pen+based+recognition+of+handwritten+digits>
data56-2 <https://archive.ics.uci.edu/dataset/81/pen+based+recognition+of+handwritten+digits>
data57 <https://archive.ics.uci.edu/dataset/39/ecoli>
data61-1 <https://archive.ics.uci.edu/dataset/54/isolet>
data62 <https://archive.ics.uci.edu/dataset/74/musk+version+1>
data63 <https://archive.ics.uci.edu/dataset/75/musk+version+2>
data64-1 <https://archive.ics.uci.edu/dataset/146/statlog+landsat+satellite>
data64-2 <https://archive.ics.uci.edu/dataset/146/statlog+landsat+satellite>
data65 <https://archive.ics.uci.edu/dataset/15/breast+cancer+wisconsin+original>
data66 <https://archive.ics.uci.edu/dataset/62/lung+cancer>
data67 <https://archive.ics.uci.edu/dataset/59/letter+recognition>
data68-1 <https://archive.ics.uci.edu/dataset/50/image+segmentation>
data68-2 <https://archive.ics.uci.edu/dataset/50/image+segmentation>
data69-1 <https://archive.ics.uci.edu/dataset/107/waveform+database+generator+version+1>
data69-2 <https://archive.ics.uci.edu/dataset/107/waveform+database+generator+version+1>
data70 <https://archive.ics.uci.edu/dataset/42/glass+identification>
data71-1 <https://archive.ics.uci.edu/dataset/148/statlog+shuttle>

| Name | URL |
|-----------|---------------------------------------------------------------------------------------------------------------------------------------------------------------------------------------------------------|
| data71-2 | https://archive.ics.uci.edu/dataset/148/statlog+shuttle |
| data72-1 | https://archive.ics.uci.edu/dataset/149/statlog+vehicle+silhouettes |
| data72-2 | https://archive.ics.uci.edu/dataset/149/statlog+vehicle+silhouettes |
| data72-3 | https://archive.ics.uci.edu/dataset/149/statlog+vehicle+silhouettes |
| data72-4 | https://archive.ics.uci.edu/dataset/149/statlog+vehicle+silhouettes |
| data72-5 | https://archive.ics.uci.edu/dataset/149/statlog+vehicle+silhouettes |
| data72-6 | https://archive.ics.uci.edu/dataset/149/statlog+vehicle+silhouettes |
| data72-7 | https://archive.ics.uci.edu/dataset/149/statlog+vehicle+silhouettes |
| data73 | https://archive.ics.uci.edu/dataset/151/connectionist+bench+sonar+mines+vs+rocks |
| data74 | https://archive.ics.uci.edu/dataset/152/connectionist+bench+vowel+recognition+deterding+data |
| NCI60 | https://github.com/natydasilva/PPforest/blob/master/data/NCI60.rda |
| crab | https://github.com/natydasilva/PPforest/blob/master/data/crab.rda |
| fishcatch | https://github.com/natydasilva/PPforest/blob/master/data/fishcatch.rda |
| glass | https://github.com/natydasilva/PPforest/blob/master/data/glass.rda |
| image | https://github.com/natydasilva/PPforest/blob/master/data/image.rda |
| leukemia | https://github.com/natydasilva/PPforest/blob/master/data/image.rda |
| lymphoma | https://github.com/natydasilva/PPforest/blob/master/data/lymphoma.rda |
| olive | https://github.com/natydasilva/PPforest/blob/master/data/olive.rda |
| parkinson | https://github.com/natydasilva/PPforest/blob/master/data/parkinson.rda |
| wine | https://github.com/natydasilva/PPforest/blob/master/data/wine.rda |

Table 6: Overview of benchmark datasets

| dataset | Cases | Predictors | Groups | Imbalance | Correlation |
|------------|-------|------------|--------|-----------|-------------|
| data12 | 329 | 12 | 6 | 0.41 | 0.38 |
| data13-1 | 122 | 13 | 2 | 0.03 | 0.41 |
| data13-2 | 121 | 13 | 2 | 0.29 | 0.37 |
| data20-1 | 2665 | 5 | 2 | 0.27 | 0.81 |
| data20-2 | 9752 | 5 | 2 | 0.58 | 0.29 |
| data20-3 | 8143 | 5 | 2 | 0.58 | 0.45 |
| data21 | 72 | 19 | 2 | 0.42 | 0.22 |
| data22-1 | 258 | 5 | 4 | 0.25 | 0.12 |
| data22-2 | 145 | 5 | 4 | 0.14 | 0.18 |
| data26 | 58 | 435 | 4 | 0.21 | 0.64 |
| data27-a11 | 1747 | 18 | 5 | 0.38 | 0.24 |
| data27-a21 | 1264 | 18 | 5 | 0.35 | 0.22 |
| data27-a31 | 1834 | 18 | 5 | 0.28 | 0.27 |
| data27-a32 | 1830 | 32 | 5 | 0.28 | 0.13 |
| data27-b11 | 1072 | 18 | 5 | 0.31 | 0.27 |
| data27-b12 | 1069 | 32 | 5 | 0.32 | 0.13 |
| data27-b31 | 1424 | 18 | 5 | 0.21 | 0.24 |
| data27-b32 | 1420 | 32 | 5 | 0.21 | 0.11 |
| data27-c11 | 1111 | 18 | 5 | 0.14 | 0.27 |
| data27-c12 | 1107 | 32 | 5 | 0.13 | 0.11 |
| data27-c31 | 1448 | 18 | 5 | 0.17 | 0.27 |
| data27-c32 | 1444 | 32 | 5 | 0.17 | 0.11 |
| data29 | 126 | 310 | 2 | 0.33 | 0.28 |
| data32 | 403 | 6 | 4 | 0.20 | 0.11 |
| data34 | 1372 | 4 | 2 | 0.11 | 0.43 |
| data36 | 210 | 7 | 3 | 0.00 | 0.61 |
| data37-1 | 29101 | 53 | 5 | 0.23 | 0.17 |
| data37-14 | 769 | 53 | 2 | 0.52 | 0.16 |
| data37-2 | 14132 | 53 | 3 | 0.62 | 0.18 |
| data37-3 | 11835 | 53 | 4 | 0.34 | 0.16 |
| data37-4 | 16357 | 53 | 5 | 0.29 | 0.15 |
| data37-5 | 17560 | 53 | 5 | 0.21 | 0.16 |

| dataset | Cases | Predictors | Groups | Imbalance | Correlation |
|----------|-------|------------|--------|-----------|-------------|
| data37-8 | 22990 | 53 | 9 | 0.27 | 0.17 |
| data38 | 182 | 12 | 2 | 0.43 | 0.21 |

| | | | | | |
|----------|------|-----|----|------|------|
| data39-1 | 445 | 128 | 6 | 0.15 | 0.55 |
| data39-2 | 1239 | 128 | 5 | 0.35 | 0.40 |
| data39-3 | 1586 | 128 | 5 | 0.17 | 0.56 |
| data39-4 | 161 | 128 | 5 | 0.32 | 0.43 |
| data39-5 | 197 | 128 | 5 | 0.22 | 0.57 |
| data39-6 | 2300 | 128 | 6 | 0.25 | 0.61 |
| data39-7 | 3613 | 128 | 6 | 0.11 | 0.68 |
| data39-8 | 294 | 128 | 6 | 0.43 | 0.57 |
| data39-9 | 470 | 128 | 6 | 0.10 | 0.42 |
| data41-1 | 5456 | 2 | 4 | 0.34 | 0.03 |
| data41-2 | 5456 | 4 | 4 | 0.34 | 0.15 |
| data41-3 | 5456 | 24 | 4 | 0.34 | 0.17 |
| data42 | 106 | 9 | 6 | 0.08 | 0.51 |
| data44 | 360 | 90 | 15 | 0.00 | 0.27 |
| data49-2 | 606 | 100 | 2 | 0.03 | 1.00 |
| data49-3 | 606 | 100 | 2 | 0.01 | 0.99 |
| data49-4 | 606 | 100 | 2 | 0.01 | 0.99 |
| data50 | 830 | 5 | 2 | 0.03 | 0.23 |
| data52-1 | 80 | 44 | 2 | 0.00 | 0.25 |
| data52-2 | 187 | 44 | 2 | 0.84 | 0.29 |
| data53 | 600 | 60 | 6 | 0.00 | 0.46 |
| data55-1 | 3823 | 64 | 10 | 0.00 | 0.12 |
| data55-2 | 1797 | 64 | 10 | 0.01 | 0.12 |
| data56-1 | 7494 | 16 | 10 | 0.01 | 0.27 |
| data56-2 | 3498 | 16 | 10 | 0.01 | 0.28 |
| data57 | 327 | 7 | 5 | 0.38 | 0.23 |
| data61-1 | 6238 | 617 | 26 | 0.00 | 0.17 |
| data62 | 476 | 166 | 2 | 0.13 | 0.26 |
| data63 | 6598 | 166 | 2 | 0.69 | 0.27 |
| data64-1 | 4435 | 36 | 6 | 0.15 | 0.49 |
| data64-2 | 2000 | 36 | 6 | 0.13 | 0.50 |
| data65 | 683 | 9 | 2 | 0.30 | 0.60 |
| data66 | 27 | 56 | 3 | 0.07 | 0.20 |

| dataset | Cases | Predictors | Groups | Imbalance | Correlation |
|----------|-------|------------|--------|-----------|-------------|
| data67 | 20000 | 16 | 26 | 0.00 | 0.18 |
| data68-1 | 210 | 19 | 7 | 0.00 | 0.30 |
| data68-2 | 2100 | 19 | 7 | 0.00 | 0.28 |
| data69-1 | 5000 | 21 | 3 | 0.01 | 0.30 |
| data69-2 | 5000 | 40 | 3 | 0.01 | 0.09 |

| | | | | | |
|-----------|-------|----|----|------|------|
| data70 | 214 | 9 | 6 | 0.31 | 0.23 |
| data71-1 | 43500 | 9 | 7 | 0.78 | 0.19 |
| data71-2 | 14494 | 9 | 5 | 0.79 | 0.20 |
| data72-1 | 94 | 18 | 4 | 0.09 | 0.39 |
| data72-2 | 94 | 18 | 4 | 0.05 | 0.40 |
| data72-3 | 94 | 18 | 4 | 0.10 | 0.42 |
| data72-4 | 94 | 18 | 4 | 0.12 | 0.42 |
| data72-5 | 94 | 18 | 4 | 0.10 | 0.49 |
| data72-6 | 94 | 18 | 4 | 0.06 | 0.40 |
| data72-7 | 94 | 18 | 4 | 0.06 | 0.44 |
| data73 | 208 | 60 | 2 | 0.07 | 0.23 |
| data74 | 990 | 12 | 11 | 0.00 | 0.22 |
| NCI60 | 56 | 31 | 7 | 0.05 | 0.56 |
| crab | 200 | 6 | 4 | 0.00 | 0.95 |
| fishcatch | 159 | 7 | 7 | 0.31 | 0.46 |
| glass | 214 | 10 | 6 | 0.31 | 0.23 |
| image | 2310 | 19 | 7 | 0.00 | 0.28 |
| leukemia | 72 | 41 | 3 | 0.40 | 0.44 |
| lymphoma | 80 | 51 | 3 | 0.41 | 0.75 |
| olive | 572 | 9 | 9 | 0.32 | 0.35 |
| parkinson | 195 | 23 | 2 | 0.51 | 0.50 |
| wine | 178 | 14 | 3 | 0.13 | 0.30 |

- Chang, Winston, Joe Cheng, JJ Allaire, Carson Sievert, Barret Schloerke, Yihui Xie, Jeff Allen, Jonathan McPherson, Alan Dipert, and Barbara Borges. 2025. Shiny: Web Application Framework for r. <https://doi.org/10.32614/CRAN.package.shiny>.
- da Silva, Natalia, Dianne Cook, and Eun-Kyung Lee. 2021. “A Projection Pursuit Forest Algorithm for Supervised Classification.” *Journal of Computational and Graphical Statistics* 30 (4): 1168–80.
- . 2025. PPforest: Projection Pursuit Classification Forest. <https://doi.org/10.32614/CRAN.package.PPforest>.
- . 2026. PPtreeExt: Projection Pursuit Classification Tree Extensions. <https://doi.org/10.32614/CRAN.package.PPtreeExt>.
- Lee, Eun-Kyung. 2018. “PPtreeViz: An R Package for Visualizing Projection Pursuit Classification Trees.” *Journal of Statistical Software* 83 (8): 1–30. <https://doi.org/10.18637/jss.v083.i08>.
- Lee, Eun-Kyung, and Dianne Cook. 2010. “A Projection Pursuit Index for Large p Small n Data.” *Statistics and Computing* 20 (3): 381–92.
- Lee, Eun-Kyung, Dianne Cook, Sigbert Klinke, and Thomas Lumley. 2005. “Projection Pursuit for Exploratory Supervised Classification.” *Journal of Computational and Graphical Statistics* 14 (4).
- Lee, Yoon Dong, Dianne Cook, Ji-won Park, Eun-Kyung Lee, et al. 2013. “PPtree: Projection Pursuit Classification Tree.” *Electronic Journal of Statistics* 7: 1369–86.

- Loh, Wei-Yin. 2014. “Fifty Years of Classification and Regression Trees.” *International Statistical Review* 82 (3): 329–48.
- Melnykov, Volodymyr, Wei-Chen Chen, and Ranjan Maitra. 2012. “MixSim: An r Package for Simulating Data to Study Performance of Clustering Algorithms.” *Journal of Statistical Software* 51 (12): 1–25.
- Therneau, Terry, and Beth Atkinson. 2025. *Rpart: Recursive Partitioning and Regression Trees*. <https://doi.org/10.32614/CRAN.package.rpart>.
- Wickham, Hadley, Dianne Cook, and Heike Hofmann. 2015. “Visualizing Statistical Models: Removing the Blindfold.” *Statistical Analysis and Data Mining: The ASA Data Science Journal* 8 (4): 203–25.
- Wickham, Hadley, Dianne Cook, Heike Hofmann, Andreas Buja, et al. 2011. “Tourr: An r Package for Exploring Multivariate Data with Projections.” *Journal of Statistical Software* 40 (2): 1–18.